Estimating the density of reef sharks from video surveys

Mathew A. Vanderklift [1*], Fabio Boschetti [1], Clovis Roubertie [1], Richard D. Pillans [2], Michael D. E. Haywood [2], Russell C. Babcock [2]

[1] CSIRO Wealth from Oceans Flagship, Private Bag 5, Wembley, 6913, Australia
[2] CSIRO Wealth from Oceans Flagship, 41 Boggo Rd, Dutton Park, 4102, Australia

[*] Corresponding author: mat.vanderklift@csiro.au

ABSTRACT

1. Policies about harvesting and conservation are developed in response to information about trends in abundance, making precise estimates of the abundance of rare and sparsely-distributed species is important.
2. Estimating the abundance of sparsely-distributed species is challenging, especially where direct observations are difficult. Reef sharks are typically sparsely distributed, and methods for making observations have distinctive biases, further complicating estimates of abundance.
3. We collected observations of reef sharks using remote underwater video cameras, and developed an agent-based model to generate estimates of the density of blacktip reef sharks (*Carcharhinus melanopterus*) from the frequency of observations made using the video. We augmented these observations with summaries of diel patterns in detections in different habitats, from *C. melanopterus* with surgically-implanted acoustic transmitters.
4. Cameras recorded higher frequencies of observation at dusk (94%) than at noon (25%). Median estimates of density from matching these observations with the agent-based model's predictions ranged from 3.5-9.9 ind/km^2 at noon to 10.7-29.5 ind/km^2 at dusk; the estimates depended on whether modelled movement paths were random or directional. These estimates suggest that individuals might exhibit diel patterns in movement, with directional movement to the reef flat during dusk. Data from tagged individuals supported this hypothesis, with more detections recorded from reef flat habitat during early evening and early morning than at other times of day.
5. Estimates of density yielded by the approach were among the highest reported in the literature for *C. melanopterus*. The agent-based model approach is flexible, and can be extended to simulate a range of behaviours, and other types of observations. Uncertainty around the estimates was high and could be reduced by increasing the density of observations, and by improving knowledge of the movement patterns of individuals.

Key-words: camera trap, *Carcharhinus melanopterus*, Lévy flight, Ningaloo, random walk, rarity, sparsely-distributed species

INTRODUCTION

Large predators can play a key role in determining the abundance and composition of their prey (Estes *et al.* 2011; Ray *et al.* 2005). As a consequence, declines in the abundance of these predators sometimes result in changes in abundance of prey, and these can further cascade down to lower trophic levels (Hairston, Smith & Slobodkin 1960; Prugh *et al.* 2009). Because of their important role in ecosystems, it is important to get accurate estimates of the abundances of large predators — a task which can be challenging, because these species are often rare, sparsely distributed or elusive, characteristics that make estimating abundance particularly difficult (Thompson 2004).

There is evidence that the abundances of many species of coastal sharks have declined, and that these declines have been followed by changes in the abundance and composition of prey (Baum *et al.* 2003; Heithaus *et al.* 2008; Myers *et al.* 2007). As a result, there have been a number of efforts to quantify the abundances of coastal sharks. The methods that are most typically used are visual censuses by divers, observations using video cameras (usually employing the use of bait as an attractant) and mark-recapture methods based on tagging. Each of these methods has its own attendant set of biases and uncertainties, and different methods can yield very different estimates of abundance (McCauley *et al.* 2012). For example, visual censuses can introduce biases associated with behavioural responses to the presence of divers, and uncertainties associated with non-instantaneous counts (Ward-Paige, Flemming & Lotze 2010), while the use of bait might yield results that vary according to the dispersal of olfactory compounds and interspecies interactions around the bait (Bassett & Montgomery 2011; Trenkel & Lorance 2011).

Because policies about harvesting or conserving sharks are influenced by advice determined — at least partly — from the results of such surveys (Techera & Klein 2011), it is important to understand the uncertainties associated with different methods, and also to attempt to use methods that best reflect the true density of sharks (i.e. the number of individual sharks per unit area). Observations made using remote underwater video cameras without bait offer perhaps the best opportunity to attain this goal, because they avoid biases that are associated with divers and bait; the cameras themselves might introduce some biases (e.g. the potential to attract or deter sharks), but any biases are likely to be minor compared to those associated with divers and bait.

However, observations made using video cameras have one critical constraint — they do not provide estimates of density. Rather, they provide information about the frequency of observation, or in some cases relative abundance. In situations in which individuals can be distinguished, capture-recapture models can be used (Marshall & Pierce 2012), but in situations in which individuals cannot be distinguished, or in which recapture rates are very low, these models are less useful. Here, we report the results of a study using an agent-based model that incorporates information about shark behaviour to provide estimates of density derived from video observations. We use this method to estimate the density of the blacktip reef shark, *Carcharhinus melanopterus*, in reef flat habitat at Ningaloo Reef (Australia) at two times of day: solar noon and just before sunset. The general approach we used involves: (i) an agent-based model of the movement tracks of individual sharks, (ii) the use of this model to estimate the frequency that sharks would be detected by video cameras (with associated uncertainty) and (iii) a comparison between this modelled frequency and the frequencies of shark observations from video camera deployments.

Estimating shark abundance in this manner is an inverse problem (Symons & Boschetti 2012; Tarantola 1987). In applied mathematics, a forward problem is one in which calculations are made based on some parameters (e.g. the density of sharks) in order to reproduce some observations (e.g. the frequency of observations of sharks from video camera deployments). We do the opposite: we use observations in order to estimate the parameters. The majority of real world problems are inverse and can rarely be solved by simple, closed-form mathematical equations (Symons & Boschetti 2012).

If the movement tracks of individual sharks could be described by simple statistics, allowing estimation of the probability of an observation of a shark at a given location, then the inverse problem described above would be fairly simple. This would occur, if for example the movement of each individual was unconstrained, for example mimicking foraging for a uniformly- or randomly-distributed resource in an essentially boundless area. This is roughly the idea on which most algorithms to establish animal abundance are based upon. However, when the movement of individuals is constrained, for example by coastline, reefs, heterogeneous habitat, interference with other individuals or recording gear or ocean currents, the probability of observing a shark at a specific location is no longer describable by a simple formula, but needs to be computed. This is what our agent-based model does.

METHOD

Study area and video camera deployments

We surveyed 16 sites in and around the Mandu Sanctuary Zone (1,185 ha) in the Ningaloo Marine Park (22° 04' S, 113° 53' E); we surveyed eight sites in the Sanctuary Zone (SZ), and eight sites in the adjoining Recreation Zone (RZ). We focused the surveys on reef flat habitat, which is typically shallow (<3 m) and dominated by tabulate coral of the genus *Acropora*. Surveys were conducted between 1-6 June 2010. We surveyed each site at two times of day — solar noon and dusk. At each site, we deployed a single video camera (Sony DCR-HC15E) in a housing mounted on a concrete block. Cameras recorded from at least 60 minutes before sunset, and at least 60 minutes following solar noon; recording times ranged from 60-94 minutes (average 87).

In the laboratory, video footage was viewed on a computer screen, and all sharks passing through the field of view were recorded. We recorded the date and time each individual shark was observed, and the amount of time spent by each individual in the field of view. From these recordings, we calculated the observed frequency of shark detection, F_{obs} as the ratio between the total time all sharks were observed in front of a camera, t_{sh}, and the total filming time, t_c.

The video camera deployments yielded 1,611 minutes of video around noon (average 89 minutes), and 1,258 minutes around dusk (average 84 minutes). Three species of carcharhinid sharks were observed (Table 1). Sharks were observed at 15 sites (94%) around dusk, and 4 sites (25%) around noon. The most frequently observed species was *Carcharhinus melanopterus*, which was observed at 13 sites (81%) around dusk, and 4 sites (25%) around noon. Subsequent modelling therefore focussed on this species.

The agent-based model

In the agent-based model, the movement of individual sharks is constrained by barriers, and is influenced by habitat. We extracted the coastline and reef crest (both barriers to movement)

from Google Earth. We represented these features, and the reef flat, in a model domain encompassing 3400 × 5050 m, with grid cells of 1 m × 1 m (Figure 1). The model requires three main components: (i) statistical distributions describing the lengths of straight-line movements and of turning angles, (ii) an algorithm controlling the way each individual interacts with habitats and obstacles to movement and (iii) a way to determine when each modelled individual can be 'detected' by the cameras in the model.

In the current implementation we do not account for how sharks interact with each other or how they interact with the video camera. However, should these behaviours be deemed important and should information about them be available, they could be included in the model.

Shark movement patterns

In our model the position of a shark at time step i, is given as

$$x_i = x_{i-1} + r_i \cos\alpha_i;\ y_i = y_{i-1} + r_i \sin\alpha_i \qquad \text{Equation 1}$$

where x and y determine the position of the shark (in Cartesian coordinates), r is the length of a straight movement performed by the shark (hereafter referred to as a step) and α is the orientation of the step. r and α are chosen stochastically from the following distributions:

$$P(r) \sim r^{-\mu} \ \ for\ r \in [minstep, maxstep] \qquad \text{Equation 2}$$

and

$$\alpha_i = \alpha_{i-1} + \theta_i$$

$$\theta_i = (1 - k_{dir})\varepsilon_i + k_{dir}\tau_i, k_{dir} \in [0,1] \qquad \text{Equation 3.}$$

In Equation 2, *P(r)* is the probability of occurrence of a step of length *r*, *minstep* and *maxstep* are the minimum and maximum step sizes, respectively (Humphries *et al.* 2010; Sims *et al.* 2008) and μ is the scaling exponent, which determines how step lengths are distributed within this range — in particular the relative distribution of small versus large steps, which determines the complexity of the path moved by each individual, as well as the total area covered in a given time interval. Ideally, μ, *minstep* and *maxstep* should be determined empirically from observations of shark movement, but such information was not available, so we chose to use *minstep* = 3 m, *maxstep* = 100 m, and three values for μ to encompass the expected range (1.7, 2 and 2.3); these values were chosen based on theoretical and empirical studies of a range of taxa, including sharks (Humphries *et al.* 2010; Sims *et al.* 2012; Sims *et al.* 2008).

Depending on the value of the exponent μ, Equation 2 reproduces two behavioural patterns commonly described in the literature: Lévy flight ($1<\mu\leq3$) and Brownian motion ($\mu>3$). Empirical observations suggest that Lévy flights are suitable for modelling foraging animal behaviour (Marell, Ball & Hofgaard 2002; Reynolds *et al.* 2007a; Reynolds *et al.* 2007b; Viswanathan *et al.* 1996), including sharks (Humphries *et al.* 2010; Sims *et al.* 2012; Sims *et al.* 2008). With $\mu\approx2$, the Lévy flight should provide an optimal search pattern (Humphries *et al.* 2010; James, Plank & Edwards 2011; Reynolds 2012; Sims *et al.* 2012; Sims *et al.* 2008; Viswanathan, Raposo & da Luz 2008) and consequently it is often assumed to be a

biologically-justified model for foraging animals. However, the choice is not critical to our approach and a different distribution could be adopted by modifying the algorithm.

In Equation 3, θ is the turning angle, defining the change of direction between two consecutive steps. Here ε_i is drawn from a uniform random distribution, and τ_i is the direction towards a desired location, in the case of oriented movement. For our discussion, the crucial parameter in this equation is $k_{dir} \in [0,1]$ which determines a balance between a fully random (k_{dir}=0) and a directional (k_{dir}=1) movement. $0.05<k_{dir}<0.3$ has been suggested to provide a realistic description of animal movement (Nams 2006). Equation 2 allows each individual to follow paths which are constrained by the distributions in Equation 3. However movement is further constrained by the coastline and model boundaries. The coastline and model boundaries are treated as 'hard' boundaries which an individual cannot cross and which require movement in the opposite direction. The rationale for treating the model boundary this way lies in the fairly short simulation time (90 minutes), which lead us to treat both the shark population and the study area as closed. Similarly, the reef crest is treated as a boundary that a shark cannot cross. We include two broad 'habitats', the reef flat habitat in which the video cameras were deployed, and the rest of the coastal waters (see Figure 1). We ran the model with k_{dir}=0, simulating unoriented Lévy flight (Bartumeus *et al.* 2002; Humphries *et al.* 2010; James, Plank & Edwards 2011; Sims *et al.* 2008; Viswanathan *et al.* 1999). and k_{dir}=0.25 which, together with τ_i yields directed movement towards the reef flat habitat (Nams 2006).

In our model sharks move at a constant speed. Because the most appropriate average swimming speed is uncertain, we used 3 values (0.5, 0.7, and 1 m/s) based on literature values for other species of carcharhinid sharks (McCauley *et al.* 2012; Sundström *et al.* 2001).

In the final step, we include cameras in the model and define the cameras' visual field (which covers an aperture angle of 90 degrees and a maximum distance from the camera of 6 metres) and record the time a shark spends within each cameras' visual field. This provides us with F_{mod}, the modelled frequency of a shark being observed;

$$F_{mod} = \frac{t_{sh}}{t_{sim} n_c} \qquad \text{Equation 4}$$

where t_{sh} is the time a shark has spent in the cameras' visual field, t_{sim} is the simulation time and n_c is the number of cameras.

Model runs and statistics of shark abundance

Because some parameters governing the shark movement (μ, speed, *minstep* and *maxstep)* were derived from estimates for related species, or from theoretical studies, we evaluated the extent to which these parameters affect the result. Preliminary simulations suggested that *minstep* and *maxstep* have a minor influence on the results (results not shown) and so we decided to fix their values to 3 m and 100 m, respectively. To account for the uncertainty in the remaining parameters, we decided to allow them to vary within ranges.

In addition to parameter uncertainty, simulation results can vary considerably between model runs due to the inherent stochasticity in the Lévy flight. In order to account for this, we ran 100 simulations for each parameter combination, resulting in 900 simulations. This gives an estimated distribution of F_{mod}.

The resulting F_{mod} is now a function of the number of simulated sharks. By calculating F_{mod} for shark populations of different sizes, we obtain F_{mod}^{s}, where s is the shark population size

for the model domain. F^s_{mod} represents the modelled distribution of shark observations, as a function of the population size, which accounts for uncertainty in our knowledge of shark behaviour as well as its inherent stochasticity.

The last step in our approach involves comparing the observations from field deployments, F_{obs} to the modelled observations, F^s_{mod}, to determine the value of *s* which provides the best match (Figure 2). For a given value of *X* (40 sharks per km^2, say), the location at which a line parallel to the *Y* axis intersects the percentile lines (80 percentile, say), gives the F^S_{mod} below which 80% of observations lies. In other words, a point (*X*, *Y*) in Figure 2 shows the percentile of models run with a density *X* of sharks which gives modelled shark observations $F^S_{mod} < Y$.

Acoustic tracking

Because the results of the agent-based modelling suggested that the best outcomes were achieved when k_{dir} was varied between noon and dusk and between reef flat and lagoon habitats (see results), we examined the results of an acoustic tagging study for evidence that this would be supported by available data. The acoustic tagging study was undertaken at Mangrove Bay (21° 57' S, 113° 56' E), approximately 10 km north of our study area. The study has been running since 2008, and a total of 60 acoustic receivers (VR2: Vemco, Canada) have been deployed over an area of approximately 28 km^2. 15 individuals of *C. melanopterus* (size range: 78-134 cm fork length) have been implanted with coded transmitters (V13 and V13, Vemco, Canada; interval between transmissions 40 or 60 seconds), following the procedure outlined in Pillans et al. (2011). We restricted the dataset to 11 individuals for which detections spanned a period of at least 100 days. We then summed all the detections by each individual into 90-minute intervals to examine diel patterns in detection. This procedure was conducted for five distinct habitats: reef flat (6 receivers, 39683 detections), lagoon (24 receivers, 80272 detections), reef slope (24 receivers, 32836 detections), reef pass (2 receivers, 7910 detections), and Mangrove Bay (4 receivers, 8629 detections).

RESULTS

In order to determine the expected density of sharks (ind/km^2) we check the modelled values of F^s_{mod} which correspond to F_{obs} (Figure 2). For k_{dir}=0 the F^s_{mod} median curve (thick line) suggests a density of approximately 29.5 ind/km^2 at dusk (80% CI: 7.9 – 68.9), and 9.9 ind/km^2 at noon (80% CI: 1.5 – 31.8). For k_{dir}=0.25 the F^s_{mod} suggests a density of approximately 10.7 ind/km^2 at dusk (80% CI: 2.3 – 23.9), and 3.5 ind/km^2 at noon (80% CI: 0.5 – 12.9).

It might be reasonable to assume that k_{dir}=0.25 at dusk (when they were more frequently observed on the reef flat) and k_{dir}=0 at noon, when sharks were assumed to not be foraging. In this case the two estimates match quite closely, with 80% confidence intervals of 2.3-23.9 ind/km^2 at dusk (median = 10.7), and 1.5-31.8 ind/km^2 at noon (median = 9.9).

Results from the acoustic receivers in Mangrove Bay provide some support to the hypothesis that individuals exhibit different movement patterns at noon and dusk; individual *C. melanopterus* were detected by receivers in reef flat habitat more frequently in the evening and in the early morning than at other times of day (Figure 3). This result would be expected if individuals were undertaking oriented movements to the reef flat at these times of day, so that k_{dir}=0.25 might be appropriate. Diel patterns in detection were observed for some of the

other habitats included in the acoustic tracking (e.g. reef slope and reef pass), but not other (e.g. lagoon).

The wide confidence intervals around the estimates of density indicate substantial uncertainty, which is partly due to uncertainty in some of the parameters used, but also to the inherent stochasticity in shark behaviour. The uncertainty can be reduced by improving the data collection and improving the statistical analysis; Appendix 1 contains a description of analyses conducted to investigate this.

DISCUSSION

The blacktip reef shark *Carcharhinus melanopterus* was the most frequently observed species of shark in the reef flat habitat, where we conducted our surveys. Our model-based method for estimating the density of *C. melanopterus* yielded estimates of 3.5-9.9 ind/km^2 at solar noon, and 10.7-29.5 ind/km^2 at dusk. These estimates are at the upper range of estimates reported by other authors (Table 2). For example, UVC surveys of 45 islands in the Pacific Ocean yielded 4 islands with estimates of >10 ind/km^2 (Nadon *et al.* 2012). The highest of these was at Palmyra, where estimates yielded 91 ind/km^2. High densities have also been reported at Aldabra (62 ind/km^2), from mark and recapture surveys (Stevens 1984). In contrast, surveys of 8 reefs on the Great Barrier Reef yielded very low estimates of density of *C. melanopterus* (Ayling & Choat 2008). Direct comparisons among these estimates are complicated by the different methods used: different methods can yield different estimates of density (McCauley *et al.* 2012), and UVC methods can yield over-estimates of density (Ward-Paige, Flemming & Lotze 2010). In addition, many of the surveys focussed on fore reef habitats, where *C. melanopterus* often occurs in low density, and other species of sharks are more abundant (Ayling & Choat 2008; Nadon *et al.* 2012) – this pattern is also observed at Ningaloo Reef (author's unpublished data).

Our surveys yielded a higher frequency of observation at dusk than at solar noon. This suggests that *C. melanopterus* might have a crepuscular (or nocturnal) pattern of habitat use, and that they use the reef flat during these periods, using other habitats (such as the sandy lagoon inshore) during the day. We have no data from other habitats with which we can test this hypothesis, but we do note that the median estimates of density at dusk with oriented movement — which would be applicable if individuals were moving towards this habitat (10.7 ind/km^2) — were similar to those obtained for noon with unoriented movement, which would be applicable if individuals were not moving towards this habitat (9.9 ind/km^2). The hypothesis that individuals exhibit different movement patterns at different times of day was supported by results yielded by detection patterns of individuals with surgically-implanted acoustic transmitters.

This pattern is also congruent with observations of other species of sharks, although data on diel patterns of density in different habitats are few. In one study, McCauley et al. (2012) found no difference in the density of sharks between day and evening. *C. melanopterus* has been observed to move into shallow habitats during a rising tide (Stevens 1984), but this does not account for our observations as the dusk surveys were conducted on a falling tide, while solar noon coincided with a rising tide.

In our model the main variables are given by μ, *minstep, maxstep,* k_{dir} and swimming speed, each of which can be altered as appropriate for different species. However, our approach does not rely on a specific model of animal behaviour, because the framework has the flexibility to accommodate different types of behaviour. An exponential distribution of step sizes,

Brownian motion or species-specific movement patterns could easily be implemented and included in the approach as appropriate.

Additional steps to implement the model in other situations include: definition of the spatial elements of the model domain (i.e. the dimensions of the area, the grid size, obstacles to movement) and how individuals behave (e.g. whether they interact with each other, with the video cameras or with map borders, whether they retain a memory of a previous path). Implementation involves decisions about the range of values associated with each parameter, such as we did for swimming speed and μ. In addition, because of the stochasticity of the model, a decision is needed about how many times to repeat each run (in our case, we chose 100 times for each combination of parameters).

Compared to traditional approaches to determine animal abundance (e.g. linear models based on data collected from visual censuses and capture-recapture models), the proposed method is time consuming to implement and to run. However, methods for estimating abundance should ideally account for patterns of animal movement and interactions with the environment. Methods which do not require the user to make decisions on these processes will inevitably take the decision for the user, in ways which are often hidden behind the maths. In such cases the user might not know how results depend on those implicit choices. The strength of the agent-based model is the flexibility it provides, as well as explicit incorporation of decisions about parameters. In addition, no assumptions are made about the distribution of individuals; for example, they can be distributed uniformly, randomly or according to some other pattern. However, if the modelled distribution F^{s}_{mod} departs substantially from a uniform distribution, effort should be allocated towards choosing a suitable statistic for comparisons with F_{obs}.

The agent-based model enabled us to generate estimates of density of blacktip reef sharks from remote underwater video observations that provided data about detection frequency. The estimates yielded by this method are among the highest reported, but have large uncertainty. Such uncertainty is common is studies of sparsely-distributed or elusive species, and can be reduced by combining methods (Gopalaswamy *et al.* 2012). Because of the ecological importance of these species, and the benefit that accurate estimates can provide to development of policies about harvesting and conservation, continued refinement of the methods is necessary.

ACKNOWLEDGEMENTS

We thank D. Thomson, K. Cook, C. Seytre and J.-B. Cazes for assistance in the field and laboratory. This research was supported by the CSIRO Wealth from Oceans Flagship and the Western Australian Department of Environment and Conservation.

REFERENCES

Ayling, A.M. & Choat, J.H. (2008). Abundance patterns of reef sharks and predatory fishes on differently zoned reefs in the offshore Townsville region: final report to the Great Barrier Reef Marine Park Authority. *Research Publication No. 91*. Great Barrier Reef Marine Park Authority, Townsville.

Bartumeus, F., Catalan, J., Fulco, U., Lyra, M. & Viswanathan, G. (2002) Optimizing the Encounter Rate in Biological Interactions: Lévy versus Brownian Strategies. *Physical Review Letters*, **88**, 2-5.

Bassett, D.K. & Montgomery, J.C. (2011) Investigating nocturnal fish populations *in situ* using baited underwater video: with special reference to their olfactory capabilities. *Journal of Experimental Marine Biology and Ecology*, **409**, 194-199.

Baum, J.K., Myers, R.A., Kehler, D.G., Worm, B., Harley, S.J. & Doherty, P.A. (2003) Collapse and conservation of shark populations in the northwest Atlantic. *Science*, **299**, 389-392.

Estes, J.A., Terborgh, J., Brashares, J.S., Power, M.E., Berger, J., Bond, W.J., Carpenter, S.R., Essington, T.E., Holt, R.D., Jackson, J.B.C., Marquis, R.J., Oksanen, L., Oksanen, T., Paine, R.T., Pikitch, E.K., Ripple, W.J., Sandin, S.A., Scheffer, M., Schoener, T.W., Shurin, J.B., Sinclair, A.R.E., Soulé, M.E., Virtanen, R. & Wardle, D.A. (2011) Trophic downgrading of planet earth. *Science*, **333**, 301-306.

Gopalaswamy, A.M., Royle, J.A., Delampady, M., Nichols, J.D., Karanth, K.U. & Macdonald, D.W. (2012) Density estimation in tiger populations: combining information for strong inference. *Ecology*, **93**, 1741-1751.

Hairston, N.G., Jr, Smith, F.E. & Slobodkin, L.B. (1960) Community structure, population control, and competition. *The American Naturalist*, **94**, 421-425.

Heithaus, M.R., Frid, A., Wirsing, A.J. & Worm, B. (2008) Predicting ecological consequences of marine top predator declines. *Trends in Ecology and Evolution*, **23**, 202-210.

Humphries, N.E., Queiroz, N., Dyer, J.R.M., Pade, N.G., Musyl, M.K., Schaefer, K.M., Fuller, D.W., Brunnschweiler, J.M., Doyle, T.K., Houghton, J.D.R., Hays, G.C., Jones, C.S., Noble, L.R., Wearmouth, V.J., Southall, E.J. & Sims, D.W. (2010) Environmental context explains Lévy and Brownian movement patterns of marine predators. *Nature*, **465**, 1066-1069.

James, A., Plank, M.J. & Edwards, A.M. (2011) Assessing Lévy walks as models of animal foraging. *Journal of the Royal Society Interface*, **8**, 1233-1247.

Marell, A., Ball, J.P. & Hofgaard, A. (2002) Foraging and movement paths of female reindeer: insights from fractal analysis, correlated random walks, and Levy flights. *Canadian Journal of Zoology*, **80**, 854-865.

Marshall, A.D. & Pierce, S.J. (2012) The use and abuse of photographic identification in sharks and rays. *Journal of Fish Biology*, **80**, 1361-1379.

McCauley, D.J., McLean, K.A., Bauer, J., Young, H.S. & Micheli, F. (2012) Evaluating the performance of methods for estimating the abundance of rapidly declining coastal shark populations. *Ecological Applications*, **22**, 385-392.

Myers, R.A., Baum, J.K., Shepherd, T.D., Powers, S.P. & Peterson, C.H. (2007) Cascading effects of the loss of apex predatory sharks from a coastal ocean. *Science*, **315**, 1846-1850.

Nadon, M.O., Baum, J.K., Williams, I.D., McPerson, J.M., Zgliczynski, B.J., Richards, B.L., Schroeder, R.E. & Brainard, R.E. (2012) Re-creating missing population baselines for Pacific reef sharks. *Conservation Biology*, **26**, 493-503.

Nams, V.O. (2006) Detecting oriented movement of animals. *Animal Behaviour*, **72**, 1197-1203.

Pillans, R., Babcock, R., Patterson, T., How, J. & Hyndes, G. (2011) Adequacy of zoning in the Ningaloo Marine Park: final report. p 123. CSIRO Marine & Atmospehric Research, Brisbane.

Prugh, L.R., Stoner, C.J., Epps, C.W., Bean, W.T., Ripple, W.J., Laliberte, A.S. & Brashares, J.S. (2009) The rise of the mesopredator. *BioScience*, **59**, 779-791.

Ray, J.C., Redford, K.H., Steneck, R.S. & Berger, J., eds. (2005) *Large carnivores and the conservation of biodiversity* Island Press, Washington.

Reynolds, A.M. (2012) Truncated Lévy walks are expected beyond the scale of data collection when correlated random walks embody observed movement patterns. *Journal of the Royal Society Interface*, **9**, 528-534.

Reynolds, A.M., Smith, A.D., Menzel, R., Greggers, U., Reynolds, D.R. & Riley, J.R. (2007a) Displaced honey bees perform optimal scale-free search flights. *Ecology*, **88**, 1955-1961.

Reynolds, A.M., Smith, A.D., Reynolds, D.R., Carreck, N.L. & Osborne, J.L. (2007b) Honeybees perform optimal scale-free searching flights when attempting to locate a food source. *Journal of Experimental Biology*, **210**, 3763-3770.

Sims, D.W., Humphries, N.E., Bradford, R.W. & Bruce, B.D. (2012) Lévy flight and Brownian search patterns of a free-ranging predator reflect different prey field characteristics. *Journal of Animal Ecology*, **81**, 432-442.

Sims, D.W., Southall, E.J., Humphries, N.E., Hays, G.C., Bradshaw, C.J., Pitchford, J.W., James, A., Ahmed, M.Z., Brierley, A.S., Hindell, M.a., Morritt, D., Musyl, M.K., Righton, D., Shepard, E.L.C., Wearmouth, V.J., Wilson, R.P., Witt, M.J. & Metcalfe, J.D. (2008) Scaling laws of marine predator search behaviour. *Nature*, **451**, 1098-1102.

Stevens, J.D. (1984) Life-histroy and ecology of sharks at Aldabra Atoll, Indian Ocean. *Proceedings of the Royal Society of London B*, **222**, 79-106.

Sundström, L.F., Gruber, S.H., Clermont, S.M., Correia, J.P.S., de Marignace, J.R.C., Morrissey, J.F., Lowrance, C.R., Thomassen, L. & Oliveira, M.T. (2001) Review of elasmobranch behavioral studies using ultrasonic telemetry with special reference to the lemon shark, *Negaprion brevirostris*, around Bimini Islands, Bahamas. *Environmental Biology of Fishes*, **60**, 225-250.

Symons, J. & Boschetti, F. (2012) How Computational Models Predict the Behavior of Complex Systems. *Foundations of Science*, **in press**.

Tarantola, A. (1987) *Inverse Problem Theory*. Elsevier, Amsterdam.

Techera, E.J. & Klein, N. (2011) Fragmented governance: reconciling legal strategies for shark conservation and management. *Marine Policy*, **35**, 73-78.

Thompson, W.L. (2004) *Sampling rare or elusive species: concepts, designs, and techniques for estimating population parameters*. Island Press, Washington.

Trenkel, V.M. & Lorance, P. (2011) Estimating *Synaphobranchus kaupii* densities: contribution of fish behaviour to differences between bait experiments and visual strip transects. *Deep Sea Research Part I: Oceanographic Research Papers*, **58**, 63-71.

Viswanathan, G.M., Afanasyev, V., Buldyrev, S.V., Murphy, E.J., Prince, P.A. & Stanley, H.E. (1996) Levy flight search patterns of wandering albatrosses. *Nature*, **381**, 413-415.

Viswanathan, G.M., Buldyrev, S.V., Havlin, S., da Luz, M.G., Raposo, E.P. & Stanley, H.E. (1999) Optimizing the success of random searches. *Nature*, **401**, 911-914.

Viswanathan, G.M., Raposo, E.P. & da Luz, M.G.E. (2008) Lévy flights and superdiffusion in the context of biological encounter and random searches. *ScienceDirect*, **5**, 133-150.

Ward-Paige, C., Flemming, J.M. & Lotze, H.K. (2010) Overestimating fish counts by non-instantaneous visual censuses: consequences for population and community descriptions. *PLoS ONE*, **5**, e11722.

Table 1: Summary of species of sharks observed, number of sites at which each was recorded, the average duration each individual spent in the field of view (in seconds, calculated only for sites at which the species was observed), and the F_{obs} for *C. melanopterus*.

	Noon			Dusk		
Species	No. sites	Ave duration	F_{obs}	No. sites	Ave duration	F_{obs}
Carcharhinus melanopterus	4	12	0.0006	13	21	0.0056
Negaprion acutidens	0	-		2	15	
Triaenodon obesus	1	7		4	5	

Table 2: Densities of *Carcharhinus melanopterus* yielded by this study and others.

Density (ind/km^2)	Method	Location	Study
9.9	Noon, k_{dir}=0	Ningaloo Reef	This study
29.5	Dusk, k_{dir}=0	Ningaloo Reef	This study
3.5	Noon, k_{dir}=0.25	Ningaloo Reef	This study
10.7	Dusk, k_{dir}=0.25	Ningaloo Reef	This study
0	UVC	Main Hawaiian Islands	Nadon *et al.* 2012
0	UVC	Northwest Hawaiian Islands	Nadon *et al.* 2012
0.04	UVC	Great Barrier Reef	Ayling & Choat 2008
0.6-8.7	UVC	American Samoa	Nadon *et al.* 2012
0-14.3	UVC	Mariana Islands	Nadon *et al.* 2012
62	Mark-recapture	Aldabra Island	Stevens 1984
0-91.2	UVC	Pacific Remote Islands	Nadon *et al.* 2012

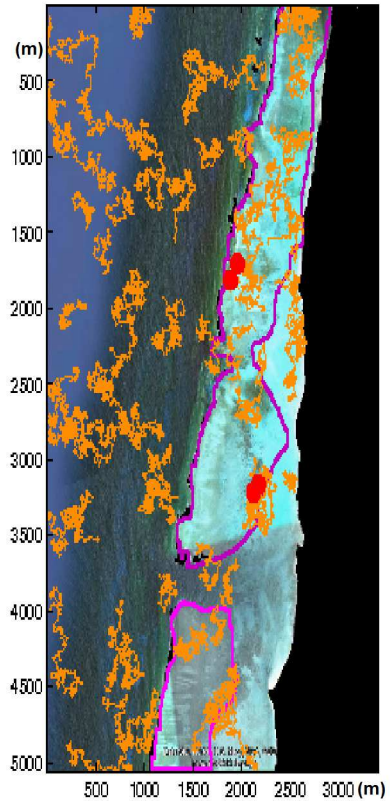

Figure 1. An example of the movement patterns reproduced by the model, showing 40 movement tracks (orange lines) for k_{dir}=0, plotted over the study area. Magenta boundaries show the reef flat habitat. Black represents land and reef crest (barriers to movement). Red dots indicate where cameras were located in field surveys.

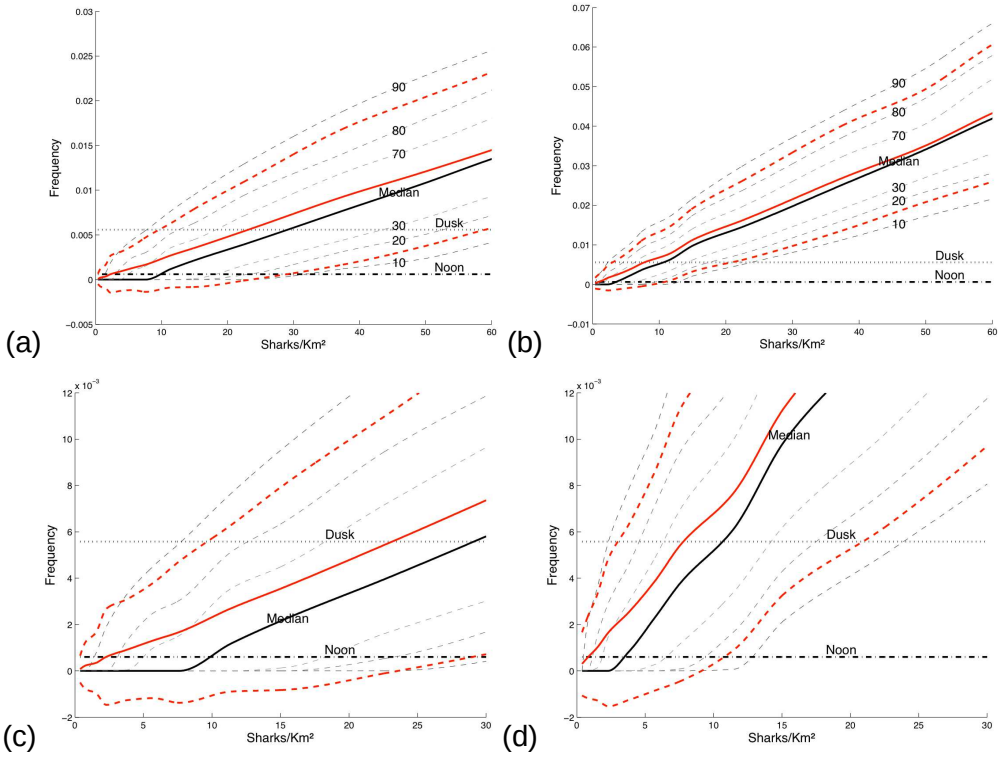

Figure 2. Modelled frequency of observations (F^{s}_{mod}) plotted against (modelled) shark density, for k_{dir}=0 (a; with lower left part of plot magnified in c) and for k_{dir}=0.25 (b, d). The *X* axis represents density *s*, (ind/km^2). The *Y* axis represents F^{s}_{mod}. The distribution of all model runs (900 runs) is represented in terms of percentiles: the thick black line corresponds to the median; dashed lines correspond to the 10, 20 ,30, 70, 80 and 90 percentiles.

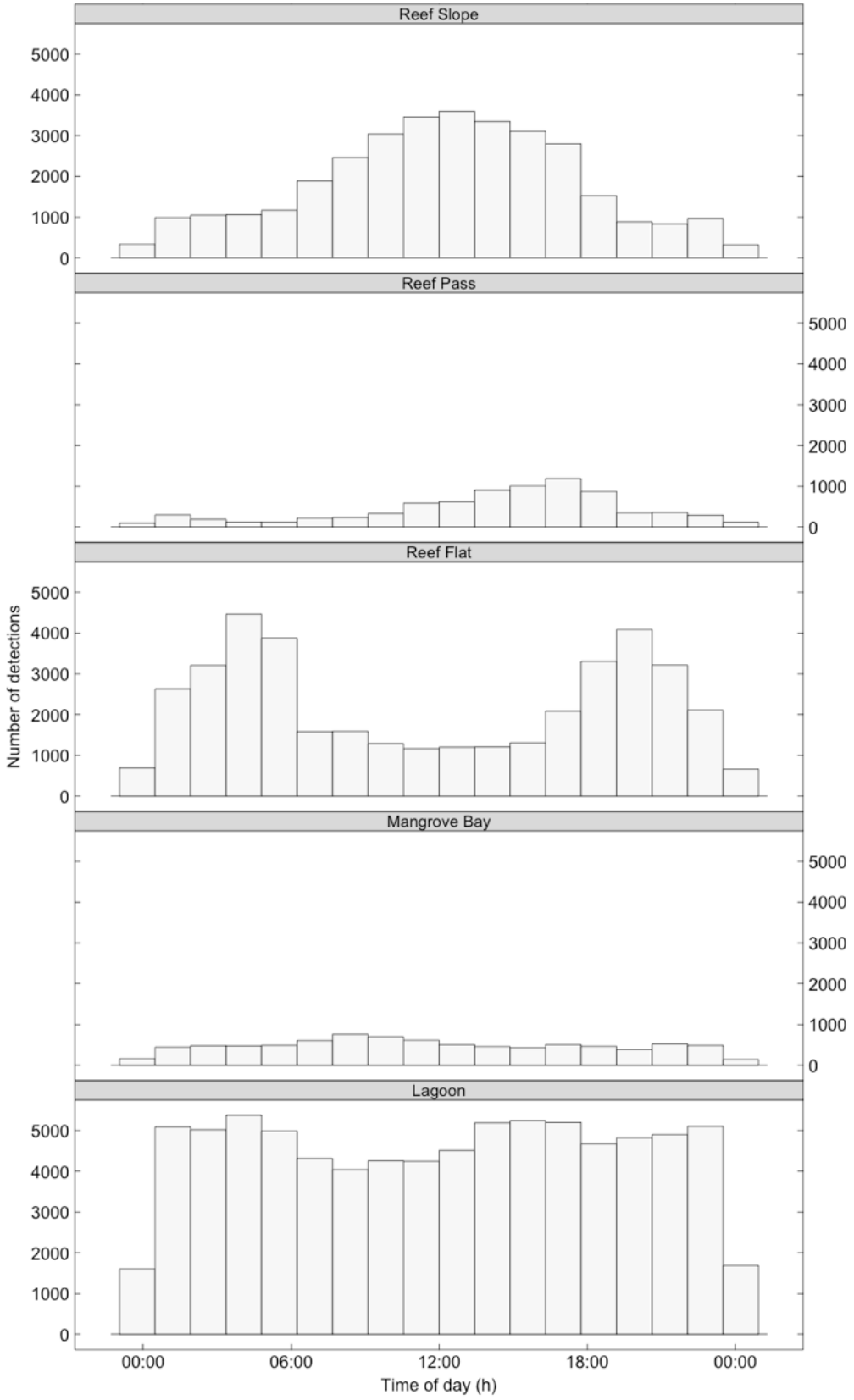

Figure 3: Total number of detections of *C. melanopterus* with surgically-implanted acoustic tags recorded by receivers in five different habitats at different times of day (binned into 90-minute categories).

Appendix 1: Description of analyses conducted to investigate sensitivity to parameter uncertainty

The uncertainty in estimates of density depends on the density of cameras (i.e. the number of cameras per unit area), the positioning of the cameras and the length of the camera recording. Increasing the density of cameras would provide more reliable estimates of the frequency of observation, but this would be nonlinear so that the relationship between the distance between cameras and the shark movement is such that further increases in camera density provides diminished returns in term of accuracy (Figure 4, Figure 5). The range between the 10^{th} and 90^{th} percentile reduces as the camera density increases (Figure 4), demonstrating that increasing camera density (e.g. from 0.3 to 2.9 cameras per km^2) increases the accuracy of the estimates of shark density.

A considerable improvement in accuracy is attained between 0.3 to 1 cameras/km^2, while further increases in camera density seem to provide diminished return in terms of accuracy. This result should be considered as problem dependent, not as a general rule, as it specifically applies to the configuration of habitats and camera locations used in our study. However, it demonstrates how the approach could be used to design a field survey.

For low shark densities (e.g. < 1.5 sharks/km^2), estimates yielded by low camera densities become unreliable (Figure 5); the 90^{th} percentiles for different camera densities intersect at low shark densities; 90^{th} percentiles converge towards infinity and the 10^{th} percentile shows a non monotonic behaviour. This pattern provides some indication for the minimum density of cameras, as a function of the expected population size, which should be used in order to obtain results of sufficient reliability. In our case, for example, we should not expect the use of a camera density below 0.25 cameras/km^2 to give reliable estimates of density when the true density is < 1.5 sharks/km^2.

The location of the camera also will affect the probability of an observation. Ideally, cameras should be positioned in such a way to increase the probability of shark detection, and doing so may require accounting for bathymetry and habitat. Figure 6 (obtained by modeling 500 individuals) illustrates this, showing an example of the how movement around obstacles could influence the spatial distribution of individuals. In situations in which unoriented movement (e.g. Brownian motion, k_{dir}=0), results in roughly similar visitation on both sides of a reef, the location of the cameras is likely to have relatively little influence on the frequency of observation (bottom left panel). The bottom right panel shows an alternative situation, in which individuals follow a Lévy flight with directional movement towards a foraging area at the right hand side (k_{dir}=0.25). In order to reach the foraging area, individuals need to move around the obstacles (e.g. reefs), which results in high visitation left of the obstacles; once they get around the obstacles, they can proceed directly to the foraging area, resulting in low visitation immediately to the right of the obstacles. Locating the cameras in different areas would result different frequencies of detection, and consequently high uncertainty around estimates of shark abundance.

In this work the duration of the model simulation was determined by the limits of the video cameras (i.e. ~90 minutes). A longer model simulation (and video recording) would increase the probability of observing sharks. However, the influence on the results depends on the animal movement within the modelled area. For a small area which can be considered as approximately closed with respect to the movement of the specific animal under study, a longer simulation time may not provide a considerable benefit, while accuracy may increase considerably in the case of a large area which is open to animal movement.

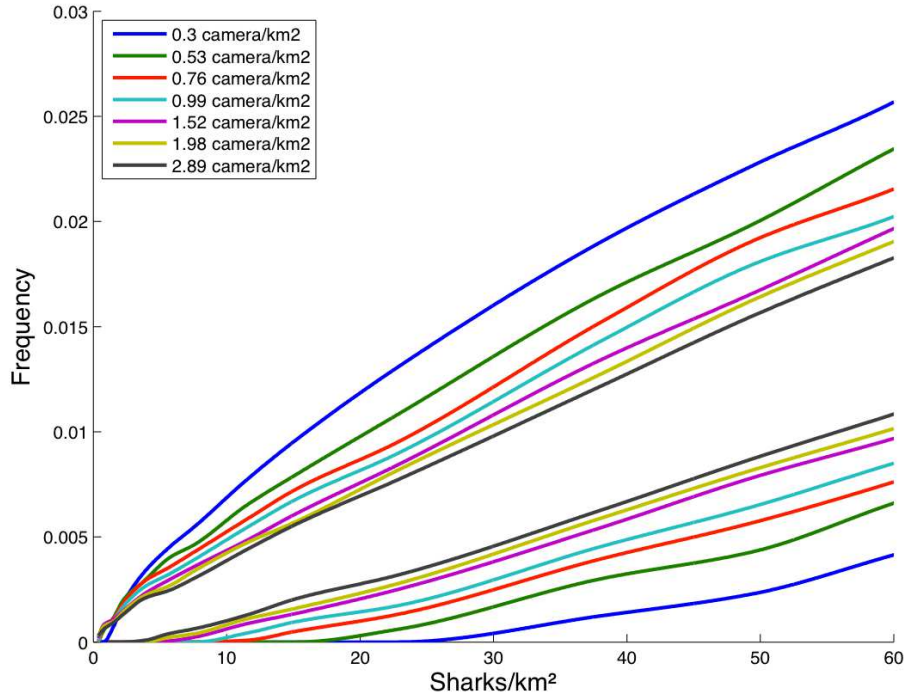

Figure 4: Modelled frequency of observations $\boldsymbol{F^{s}_{mod}}$ plotted against shark densities for different camera densities, for k_{dir}=0. The 10th and 90th percentiles of the distributions for each camera density are shown. Colours refer to camera densities ranging from 0.3 to 2.9 cameras per square kilometres.

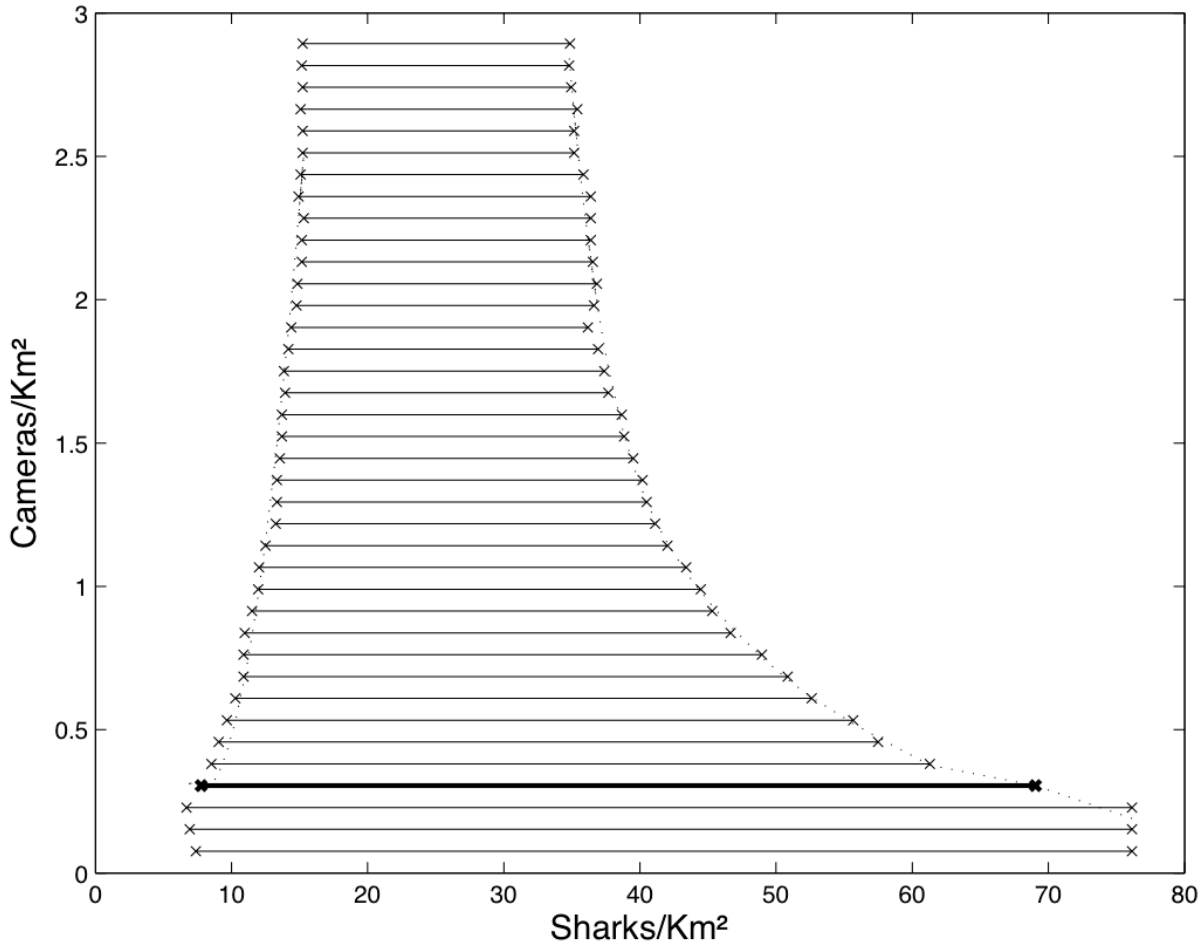

Figure 5: Camera density plotted against shark density k_{dir}=0. Plot shows the range between the 10 and 90 percentiles. Thick black line represents the densities of cameras used in our study (0.3 cameras per km^2).

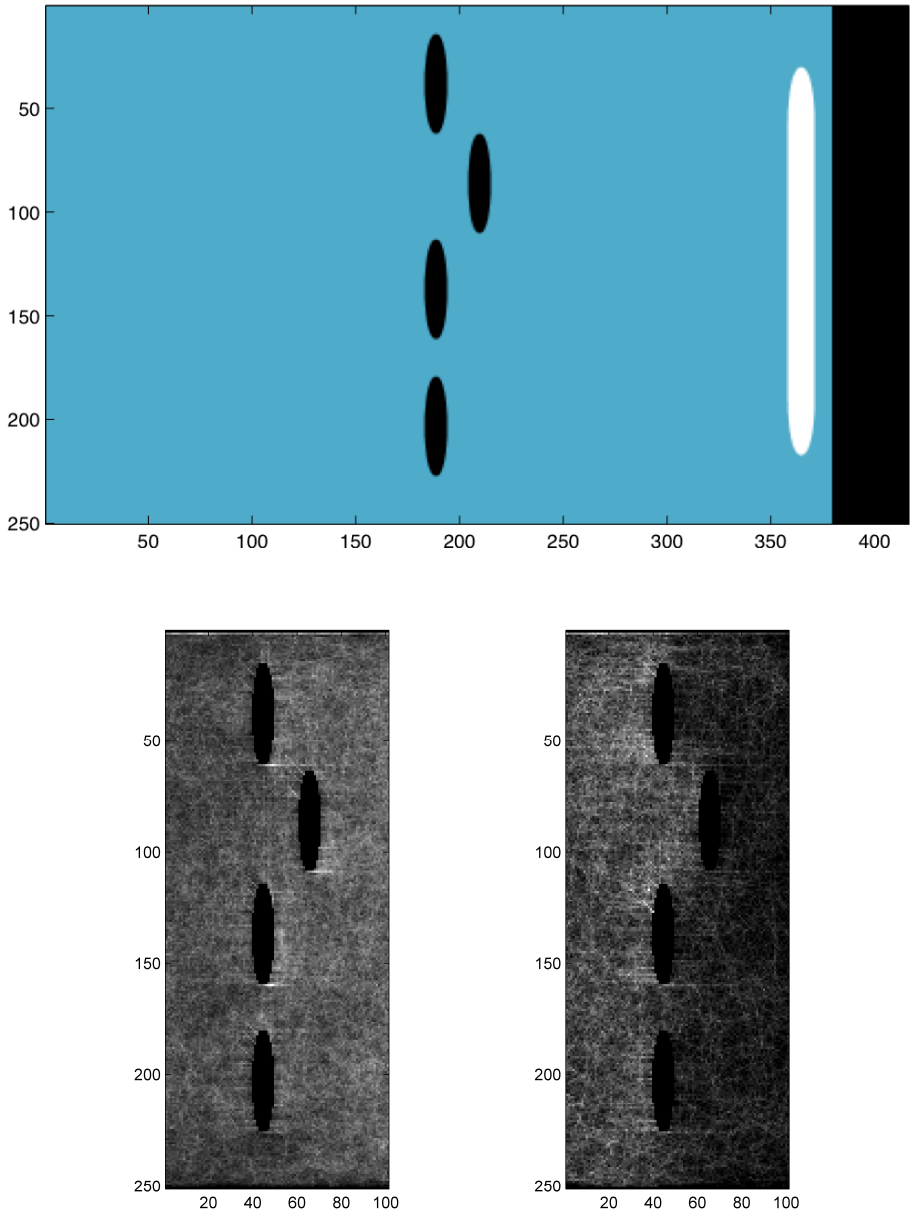

Figure 6: An example of the impact of how movement patterns can influence spatial distribution, and therefore the probability of detection, obtained by modelling movement for 500 individuals. Top panel shows a simplified model domain: black areas represent obstacles (e.g. coast and reefs), the white area represents a foraging area. The bottom left panel shows the result of simulations with unoriented movement (k_{dir}=0), and the bottom right panel shows the result of simulations with oriented movement (k_{dir} =0.25); shading show the number of times individuals cross each pixel (dark=high visitation).